JOURNAL DE PHYSIQUE IV
Colloque C8, supplément au Journal de Physique III, Volume 5, décembre 1995

Analysis of Microstructures in Cu-14.0%Al-3.9%Ni by Energy Minimization

C. Chu and R.D. James

Department of Aerospace Engineering and Mechanics, 107 Akerman Hall, 110 Union Street S.E., University of Minnesota, Minneapolis, MN 55455, U.S.A.

Abstract. During the past few years, a new theory of martensite has been developed in which microstructure is predicted by energy minimization ([1, 2]). The theory is based on a crystallographic model, and the continuum theory is obtained from this model by using the Cauchy-Born rule to relate atomic to macroscopic deformation. The theory treats the geometry of deformation exactly, regardless of the size of the transformation strain. The authors believe that this theory could be widely used by experts on martensite to analyze and predict microstructures. To illustrate one way the theory can be used, the authors take several of the commonly observed microstructures in CuAlNi and show how each of them can be obtained directly by energy minimization of a given energy function. In particular, we consider the austenite-martensite interface (the theory subsumes the crystallographic theory of martensite), the divided wedge, laminates of compound twins, layers within layers of Type II twins, and simple and complex twin crossings. In each of these cases the theory gives precise information on deformed geometry, orientation of interfaces, and volume fractions.

1. THEORY OF MARTENSITE

In recent years a geometrically nonlinear theory of martensitic transformations has been developed in which microstructures are identified with "minimizing sequences." This theory is based on a crystallographic picture, and the passage to continuum level is made via the Cauchy-Born rule. A key part of the crystallographic derivation is the identification of a region in the space of lattice vectors (the Ericksen- Pitteri neighborhood) on which a consistent symmetry group acts. It is not the purpose of this paper to repeat this derivation, which can be found in [2], but rather to show how the results can be used to understand the presence of microstructure. To do this economically, we focus on a single material (the well-known Cu-14.0%Al-3.9%Ni), describe its free energy function, and analyze its commonly observed microstructures. While we think this gives a good sense of what the theory can and cannot do, it does not highlight the the most important uses of the theory: 1) to predict new microstructures, 2) to predict behavior. For some aspects of the latter, see [2]. For this short paper we are not able to give all the details of the solutions of the equations in each case. Here we give an overview and concentrate on the results.

The basic unknowns of the theory are deformations, represented by functions $\mathbf{y}(\mathbf{x})$, $\mathbf{x} \in \Omega$. The reference configuration Ω represents undistorted austenite. The total free energy of the material (without loads applied) is given by,

$$\int_{\Omega} \varphi\left(\nabla \mathbf{y}(\mathbf{x}), \theta\right) d\mathbf{x} \tag{1}$$

Here, φ is the free energy density as a function of the deformation gradient $\mathbf{G}$ (a 3×3 matrix) and temperature θ. From the principle of frame-indifference φ must satisfy $\varphi(\mathbf{RG}, \theta) = \varphi(\mathbf{G}, \theta)$ for all rotation matrices $\mathbf{R}$, i.e. 3×3 matrices in the set $SO(3) = \{\mathbf{R} : \mathbf{R}^T\mathbf{R} = \mathbf{1},\ \det \mathbf{R} = +1\}$, and all temperatures θ. We shall use the notation $SO(3)\mathbf{A}$ to denote all matrices of the form $\mathbf{RA}$, where $\mathbf{R} \in SO(3)$, denoted here by a circle attached to $\mathbf{A}$:

SO(3)A = 

For this paper we will only need to describe the energy wells of φ. We also focus on the β_1 to γ_1' transformation only (The treatment of the β_1 to β_1' transformation adds additional energy wells at larger strains; see Bhattacharya [4], forthcoming). Let θ_c denote the transformation temperature of the material, defined as the temperature at which the undistorted austenite and martensite phases have equal free energy density. The energy wells are defined in terms of the six matrices,

$$\mathbf{U}_1 = \begin{pmatrix} \frac{\alpha+\gamma}{2} & \frac{\alpha-\gamma}{2} & 0 \\ \frac{\alpha-\gamma}{2} & \frac{\alpha+\gamma}{2} & 0 \\ 0 & 0 & \beta \end{pmatrix}, \quad \mathbf{U}_3 = \begin{pmatrix} \frac{\alpha+\gamma}{2} & 0 & \frac{\alpha-\gamma}{2} \\ 0 & \beta & 0 \\ \frac{\alpha-\gamma}{2} & 0 & \frac{\alpha+\gamma}{2} \end{pmatrix}, \quad \mathbf{U}_5 = \begin{pmatrix} \beta & 0 & 0 \\ 0 & \frac{\alpha+\gamma}{2} & \frac{\alpha-\gamma}{2} \\ 0 & \frac{\alpha-\gamma}{2} & \frac{\alpha+\gamma}{2} \end{pmatrix},$$

$$\mathbf{U}_2 = \begin{pmatrix} \frac{\alpha+\gamma}{2} & \frac{\gamma-\alpha}{2} & 0 \\ \frac{\gamma-\alpha}{2} & \frac{\alpha+\gamma}{2} & 0 \\ 0 & 0 & \beta \end{pmatrix}, \quad \mathbf{U}_4 = \begin{pmatrix} \frac{\alpha+\gamma}{2} & 0 & \frac{\gamma-\alpha}{2} \\ 0 & \beta & 0 \\ \frac{\gamma-\alpha}{2} & 0 & \frac{\alpha+\gamma}{2} \end{pmatrix}, \quad \mathbf{U}_6 = \begin{pmatrix} \beta & 0 & 0 \\ 0 & \frac{\alpha+\gamma}{2} & \frac{\gamma-\alpha}{2} \\ 0 & \frac{\gamma-\alpha}{2} & \frac{\alpha+\gamma}{2} \end{pmatrix},$$

where $\alpha = 1.0619$, $\beta = 0.9178$ and $\gamma = 1.0230$ for this alloy. It turns out from the theory that there are seven energy wells at $\theta = \theta_c$. That is, $\varphi(\mathbf{G}, \theta_c) \geq 0$ and $\varphi(\mathbf{G}, \theta_c) = 0$ precisely on the set:

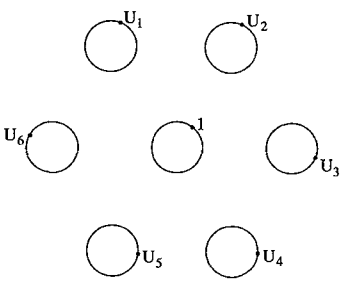

For $\theta > \theta_c$, φ is minimized just at the *austenite well* $SO(3)\alpha(\theta)\mathbf{1}$, while for $\theta < \theta_c$ the *martensite wells* $SO(3)\mathbf{U}_1 \cup \ldots \cup SO(3)\mathbf{U}_6$ are at lowest energy. Here $\alpha(\theta)$, $\alpha(\theta_c) = 1$, describes thermal expansion of the austenite.

2. MINIMIZING SEQUENCES

To minimize the total free energy appropriate to an unloaded single crystal, we fix θ and minimize (1) over all deformations. We assume such deformations are continuous but that the deformation gradients may have jump discontinuities that model for example twin interfaces ("fiducial scratches can bend sharply but never break"). The energy (1) has a strange property first noticed by L.C. Young in the 1930's for simple minimization problems. That is, for certain boundary value problems (see [2] for examples) the minimum energy in (1) is not attained. This means that the total energy is bounded below (as in the case of our φ) but that *there is no deformation that one can put into the total energy that actually achieves this minimum energy.* From the form of (1) there are always minimizing sequences, that is, sequences of deformations $\mathbf{y}^{(k)}(\mathbf{x})$, $k = 1, 2, 3, \ldots$ that make the total energy closer and closer (as $k \to \infty$) to its minimum value, and one is led in this situation to study them. Necessarily they involve finer and finer features as k gets larger and larger, and the idea is that these model fine microstructures. Nonattainment is a tip-off to something more basic (the failure of "weak lower semicontinuity"), which in turn indicates that *even when there is attainment*, one should study the minimizing sequences. One may get the impression by looking at the arguments below that minimizing sequences are rather arbitrary, but, in fact, the condition that they are minimizing places strong restrictions on the possible constructions.

Our minimizing sequences will be based on three such constructions. The first will be twin interfaces in which $\nabla \mathbf{y}^{(k)}(\mathbf{x})$ alternates between two matrices $\mathbf{A}$ and $\mathbf{B}$, on bands of width $1/k$ separated by interfaces with normal $\mathbf{n}$, and the volume fraction of the region where $\nabla \mathbf{y}^{(k)}(\mathbf{x}) = \mathbf{A}$ being λ. Such a deformation is continuous if $\mathbf{A} - \mathbf{B}$ is a rank-one matrix: $\mathbf{A} - \mathbf{B} = \mathbf{a} \otimes \mathbf{n}$ (Here $\mathbf{a} \otimes \mathbf{n}$ is a matrix with components $a_i n_j$).

Augmenting our notation, a straight line drawn between two matrices will always mean that they differ by a matrix of rank 1 (below, right):

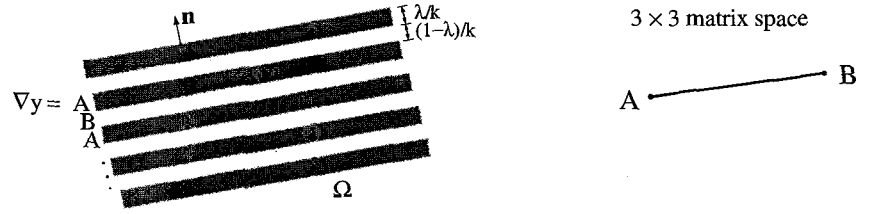

Figure 1. A simple laminate with alternating deformation gradients **A** and **B** (left) and the associated rank-1 connection.

For this sequence to be minimizing, **A** and **B** must lie on the energy wells at the appropriate temperature (In fact, each member of this sequence has minimum energy in this case). Another construction (closely related to the crystallographic theory of martensite) is alternating bands with gradients **A** and **B** and the volume fraction λ, meeting a homogeneous deformation with gradient **C** at a transition layer (shaded), of width $1/k$, viz.

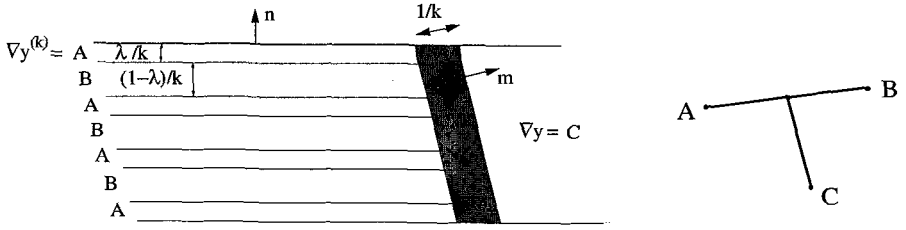

Figure 2. A laminate meeting a homogeneous deformation (left) and the associated rank-1 connections (right).

For this sequence of deformations, it is necessary to construct a deformation defined on the transition layer, in the spirit of the WLR theory [8], and this is easily done (Note, however, that in the WLR theory, free energy changes are not considered). The gradient in this transition layer can be made bounded (independent of k) if and only if certain compatibility conditions are satisfied by the three matrices **A**, **B**, and **C**, and these are given by Figure 2 (right). We have extended the notation further: a line meeting another as shown above means that $(\lambda\mathbf{A} + (1-\lambda)\mathbf{B}) - \mathbf{C} = \mathbf{b} \otimes \mathbf{m}$, for some vectors $\mathbf{b}$ and $\mathbf{m}$, i.e. that **C** is rank-1 connected to a matrix on the line between **A** and **B**. Implicit in this notation is that the fractional distance along this line is the volume fraction λ that is used in the construction. Since the deformation gradient in the transition layer is bounded, and the layer volume goes to 0 as $k \to \infty$ then, by the form of (1), this is a minimizing sequence, as long as **A**, **B**, and **C** lie on the energy wells (There are various ways to do this, giving rise to various microstructures).

Finally, there are sequences that model laminates meeting laminates. Again there is a transition layer between the laminates whose energy must go to zero, and this gives rise to compatibility conditions between the deformation gradients. The result is:

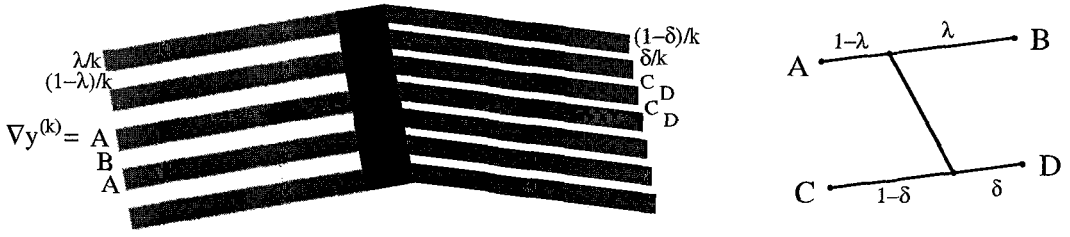

Figure 3. Compatibility conditions for laminates meeting laminates.

3. GEOMETRY OF DEFORMATIONS

The geometry of microstructure is represented by the deformation $\mathbf{y}^{(k)}(\mathbf{x})$ with k large. A picture like the simple laminate shown above with gradients $\mathbf{A}$ and $\mathbf{B}$ is a picture in the reference configuration Ω, showing the $\mathbf{x}$ values where $\nabla\mathbf{y}^{(k)}(\mathbf{x})$ takes on various matrices. However, when we view the microstructure, we see interfaces and volume fractions in the deformed configuration. That is, for this simple laminate, the observed interfaces will not have normal $\mathbf{n}$ but instead will have whatever normal is obtained by plotting the image of the interfaces under $\mathbf{y}^{(k)}(\mathbf{x})$. There are standard formulas of "continuum mechanics" that relate reference and deformed quantities like normals to interfaces and transition layers, and volume fractions. For example, the deformed normal corresponding to the simple laminate is proportional to $\mathbf{A}^{-T}\mathbf{n}$ (which, by the condition $\mathbf{A}-\mathbf{B}=\mathbf{a}\otimes\mathbf{n}$ is also proportional to $\mathbf{B}^{-T}\mathbf{n}$). When we say below that a microstructure agrees well with the pictured one, we mean that when we calculate the *deformed* normals to interfaces and transition layers, these agree within $\pm 2°$ (our typical error of orientation) and volume fractions (away from transition layers) within $\pm 5\%$ with the experimental pictures. See [3] for more details.

4. SPECIAL MICROSTRUCTURES

4.1 Austenite/martensite interface

This microstructure, pictured in Figure 4 (left), is well understood and we add little to what is known. The associated sequence and the conditions for this sequence to be minimizing are given in Figure 2 specialized to $\mathbf{A}$ and $\mathbf{B}$ on the martensite wells and $\mathbf{C}=\mathbf{1}$. Solving the system of equations represented by these rank-1 connections, one gets the possible volume fractions and normals exactly as given by the crystallographic theory of martensite. There are three minor advantages of the present approach: 1) the twinning system does not have to be assumed, as it comes out automatically by solving for the rank-1 connection between $\mathbf{A}$ and $\mathbf{B}$, 2) there is a conceptual advantage of separating the compatibility calculation (represented by the "T" in Figure 2 (right)) from the part of the calculation that places $\mathbf{A}$ and $\mathbf{B}$ and $\mathbf{C}$ on the wells, and 3) it can be proved in the present context that any minimizing sequence that essentially uses three matrices, with one matrix not rank-1 connected to the other two, must look essentially like Figure 4 (left) and in particular must exhibit fine, macroscopically periodic twins meeting a plane transition layer [7].

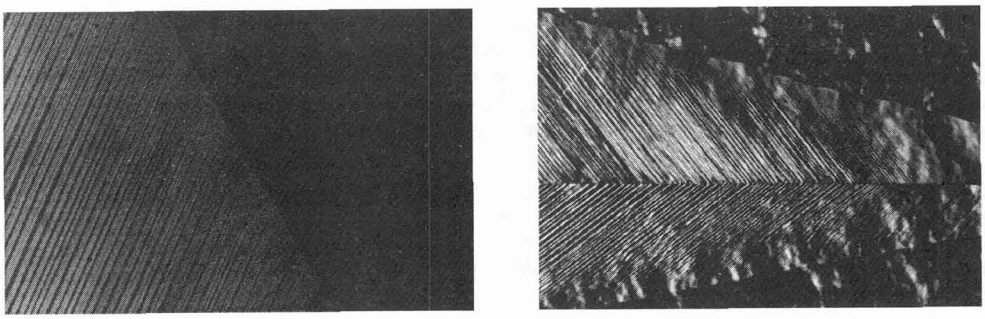

Figure 4. Austenite/martensite interface (left) and wedge (right).

4.2 Divided wedge

This microstructure has been analyzed by Bhattacharya [3] so we just summarize briefly. The structure of the minimizing sequence and the rank-1 connections are shown below.

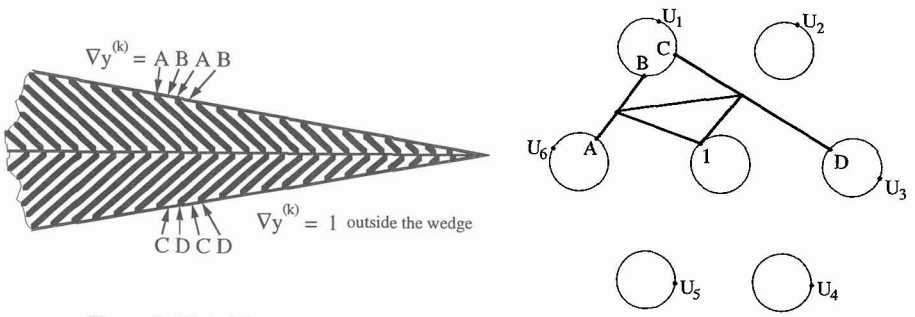

Figure 5. Minimizing sequence for the divided wedge and associated rank-1 connections.

The symmetric shape of the wedge, the equality of volume fractions in either half and its value, the fact that Type I twins in wedges point forward and Type II backward, and the impossibility of wedges formed from compound twins are predicted by solving the rank-1 connections listed above. The theory does not explain why Type II wedges are more common than Type I wedges. Conceptually, this microstructure is extremely important for the following reason: the rank-1 connections shown in Figure 5 can *only* be satisfied if there is a special relation among lattice parameters, $f(\alpha, \beta, \gamma) = 0$ [3]. This relation, which is satisfied very closely by the Cu-14.0%Al-3.9%Ni alloy under study, does not follow from symmetry. This establishes a direct link between special microstructures and special lattice parameters.

4.3 Laminates of compound twins

Compound twins form patches as shown below (left) especially during variant rearrangement.

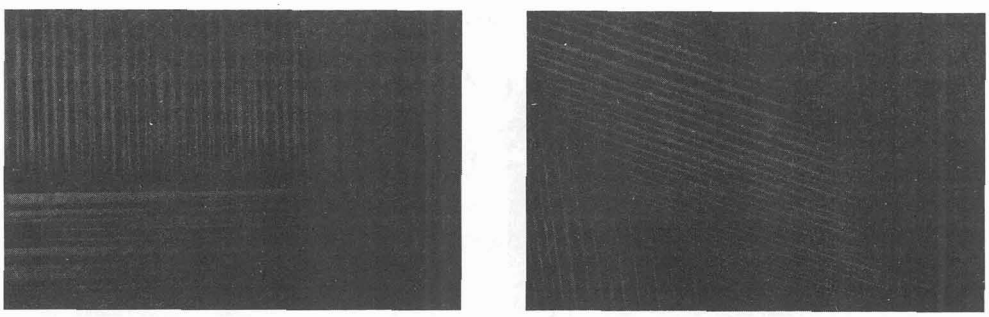

Figure 6. Laminates of compound twins (left) and layers within layers of Type II twins (right).

This is just like two austenite/martensite interfaces, except the deformation gradients **B** and **D** lie on one of the two compound twinned martensite wells:

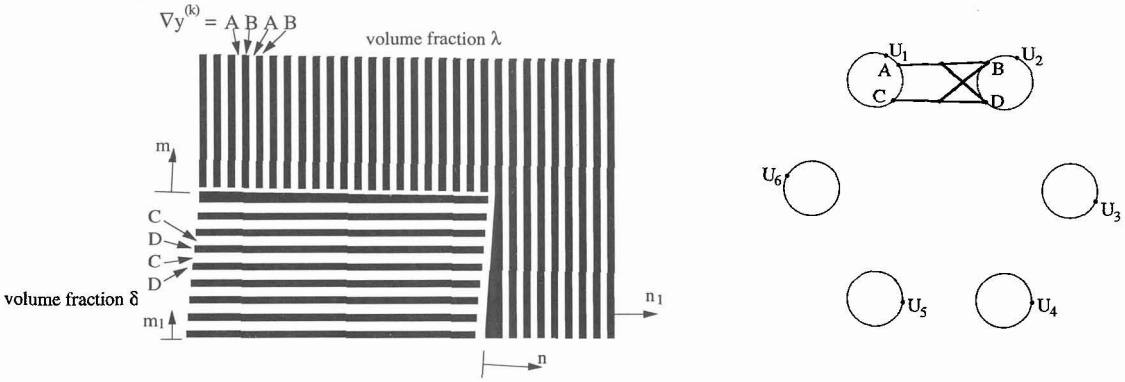

Figure 7. Minimizing sequence and rank-1 connections for compound twinned laminates.

It follows necessarily from this calculation that normals $\mathbf{m}$ and $\mathbf{n}$ to the transition layers are very close to the twin normals $\mathbf{m}_1$ and $\mathbf{n}_1$, in agreement with Figure 8. However, unlike the austenite- martensite interface, the above is a minimizing sequence for any volume fraction λ between 0 and 1, as is observed, suggesting why this microstructure is seen during variant rearrangement.

4.4 Layers within layers of Type II twins

This microstructure, shown in Figure 6 (right), is commonly produced in the wake of a set of parallel, propagating wedges. The associated rank-1 connections are really a special case of those for the divided wedge.

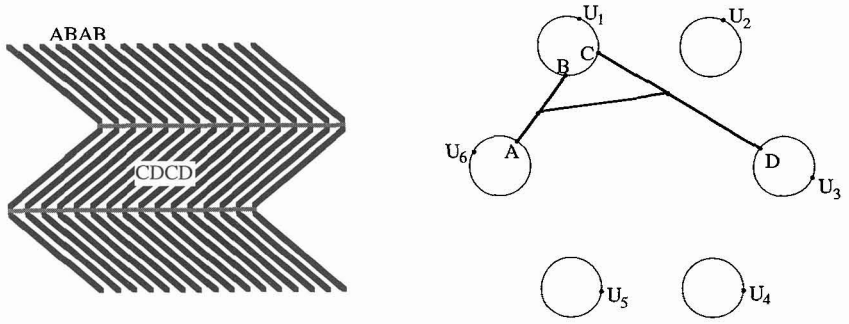

Figure 8. Minimizing sequence and rank-1 connections for the layers within layers.

4.5 Simple and complex twin crossings

A simple microstructure seen in Cu-Al-Ni is the twin crossing (Figure 9, left). It appears as shown with one twin passing straight through, and often forms more complicated checkerboard patterns. More complex twin crossings are shown in Figure 9, right.

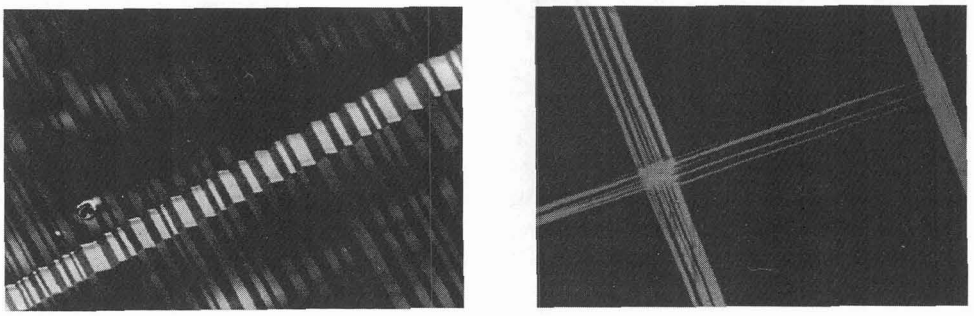

Figure 9. Simple and complex twin crossings.

The set of rank-1 connections that allow these microstructures to be energy minimizing are shown below.

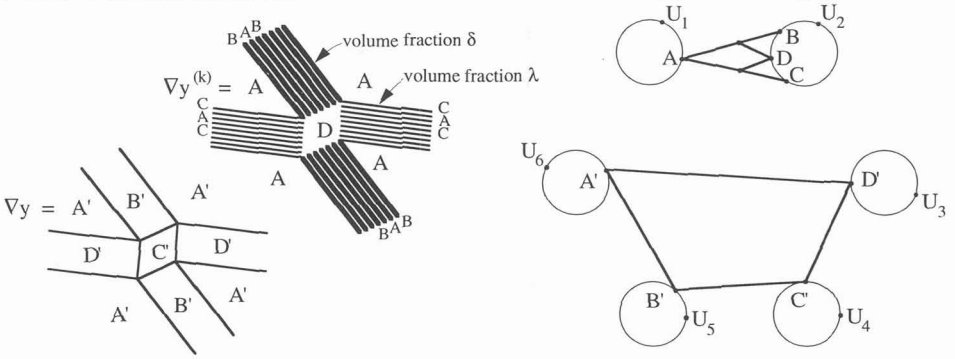

Figure 10. Minimizing sequences and rank-1 connections for simple and complex twin crossings.

The geometry that follows by solving for these rank-1 connections comes out as shown in Figure 9. In particular, for the complex twin crossing, the volume fractions necessarily satisfy the conditions $\delta = 1 - \lambda$ but λ can have any value between 0 and 1. This is roughly seen in Figure 9 (right), though one also sees the limitations of the theory. It should be emphasized that the rank-1 connections of Figure 10 are more restrictive than geometry: it is possible to draw several hypothetical twin crossings that use the natural twin normals between variants, but only a few of these are actually compatible (see [5, eqn (160)] for sufficient conditions for a twin crossing).

Acknowledgement

The authors thank ONR (N00014-93-1-0240, N00014-91-J-4034), AFOSR (AFOSR-91-0301) and NSF (CMS-95-03633, DMS-9111572-02) for supporting this work.

References

[1] Ball J.M. and James R.D., *Archive for Rational Mechanics and Analysis* **100** (1987), pp. 13–52.
[2] Ball J.M., and James R.D., *Phil. Trans. Royal Soc. London A.* **338** (1992), pp. 389–450.
[3] Bhattacharya K., *Acta. Met.* **219** (1991), pp. 2431–2444.
[4] Bhattacharya K., in preparation.
[5] Chu C. and James R.D., in preparation.
[6] James R.D. and Kinderlehrer D., *Phil. Mag. B.* **68** (1993), pp. 237–274.
[7] James R.D. and Kinderlehrer D., *Lecture Notes in Physics* **344** (1990), pp. 57.
[8] Wechsler M.S., Lieberman D.S. and Read T.A., *Trans. AIME J. Metals* **197** (1953), pp. 1503–1515.